International Journal of Sciences and Techniques of Automatic control & computer engineering
IJ-STA, Volume 2, N° 2, December 2008, pp. 790–803.

Performance of a Sensorless Direct Torque Flux Control Strategy for Induction Motors associated to the three levels NPC Converter used in Electric Vehicles

Ahmed Abbou and Hassane Mahmoudi

Département Génie Electrique
Laboratoire d'Electrotechnique et d'Electronique de Puissance
Ecole Mohammadia d'ingénieurs
Avenue Ibn Sina B.P. 767 Agdal Rabat, Morocco.
Abbou2010@hotmail.com - *mahmoudi@emi.ac.ma*

Abstract. *This paper presents the performance of a Sensorless direct torque and flux control (DTFC) of induction motor (IM) associated to the three level neutral-point-clamped (NPC) converter. The motor is a three phase squirrel-cage used as a propulsion system of an electric vehicle. We estimated the speed by using the model reference adaptive system (MRAS). The regulator of speed used is a P-PI type. The control method proposed in this paper can reduce the flux ripples and the torque and especially improve the performances of the DTFC strategy in high and low speeds.*

Keywords. *Sensorless drive***,** *IM, DTFC, MRAS, (P-PI) Regulator, Three levels NPC converter.*

Résumé. *Ce papier présente les performances de la stratégie de commande contrôle direct de flux et de couple (DTFC) sans capteur de vitesse pour un moteur à induction (IM) associée à un onduleur de tension trois niveaux de type NPC. Le moteur étudié est triphasé à cage d'écureuils en vue de l'utiliser dans un véhicule électrique. Pour estimer la vitesse de rotation, on a utilisé un système adaptatif utilisant le modèle de référence (MRAS). Le régulateur de vitesse est de type (P-PI). Cette stratégie de commande proposée permet de réduire les ondulations de flux et de couple et assure de bonnes performances en basses vitesses et en survitesses.*

Mots-clés. *Commande sans capteur***,** *IM, DTFC, MRAS, Régulateur (P-PI), onduleur trois niveaux de type NPC.*

1. Introduction

The electric vehicle represents a potential solution for our future, helping to advancing the resolution of environmental problems caused by combustion motors. Three-phase squirrel cage-rotor induction motors are best suited to electric vehicle drive applications. Induction motors are cost-effective, and are suitable in terms of size and weight, speed of rotation, efficiency, controllability and reliability. The durable rotor and high speed operation which are easily implemented with a field-weakening control enable the use of large reduction gear ratios that limit maximum torque requirements, and allow using smaller motors driven by compact low current inverters.

Furthermore, the strategy of the direct torque and flux control is currently knowed as the technique the most often employed when controlling induction motors. The use of these orders is associated with the high-quality dimensionality of the parameters of the regulators, which permit us to recover the suppleness of control and the quality of the electromechanical conversion for the induction machine, found naturally with the DC machine.

For economical and maintenance reasons, the Sensorless control constitutes one of the main preoccupations of the industrial. Also, Neutral-point-clamped converters are increasingly used in industrial drive systems as they allow to use of lower voltage devices in higher voltage applications, provide lower output voltage total harmonic distortion (THD) [2], and can develop low common mode voltage.

2. Direct Torque and Flux Control

Direct Torque and Flux Control (DTFC) method was introduced in 1985 by I. Takahashi and M. Depenbrock [9]. This strategy of control is relatively new and competitive compare to the Rotor Flux Oriented method [7]. This method presents the advantage of a very simple control scheme of stator flux and torque by two hysteresis controllers, which give the input voltage of the motor by selecting the appropriate voltage vectors of the inverter through a look-up-table in order to keep stator flux and torque within the limits of two hysteresis bands as shown in Fig.1. The application of this principle allows a decoupled control of flux and torque without the need of coordinate transformations, PWM pulse generators and current regulators.

The block diagram of an induction motor drive controlled with direct torque and flux control strategy is drawn in Fig. 1.

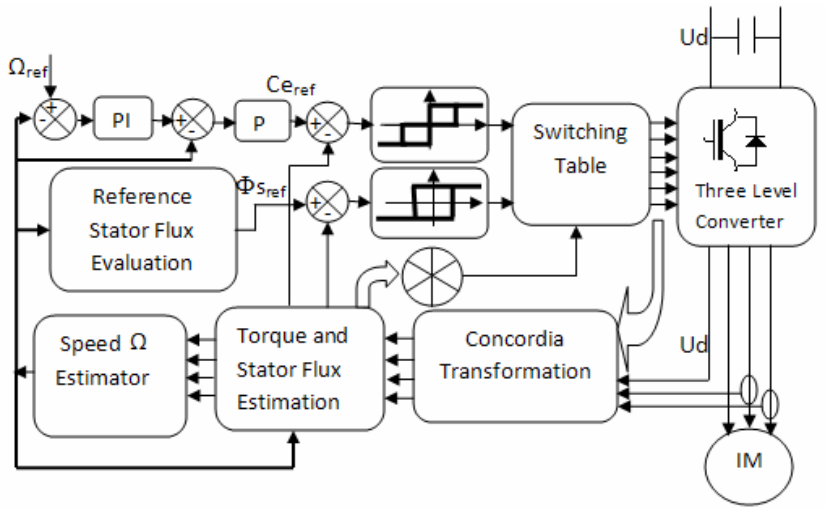

Fig.1. DTFC block diagram

The vector tension Vs come from a three level converter, whose switches are controlled by Boolean's four sizes of Sij order (i=1, 2, 3, 4 and j=A, B, C).
The stator flux, as given in equation (1), can be approximated as equation (2) over a short time period if the stator resistance is ignored.

$$\overline{\Phi}_s = \overline{\Phi}_{so} + \int_0^t (\overline{V}_s - R_s \overline{I}_s)dt \quad (1) \qquad \overline{\Phi}_s \approx \overline{\Phi}_{so} + \int_0^t \overline{V}_s dt \quad (2)$$

During one period of sampling Te, vector tension applied to the machine remains constant, and thus one can write:

$$\overline{\Phi}_s(k+1) \approx \overline{\Phi}_s(k) + \overline{V}_s.T_e \quad (3) \qquad \text{Or} \quad \Delta\overline{\Phi}_s \approx \overline{V}_s.T_e \quad (4)$$

Therefore to increase the stator flux, we can apply a vector of tension that is co-linear in its direction and vice-versa.

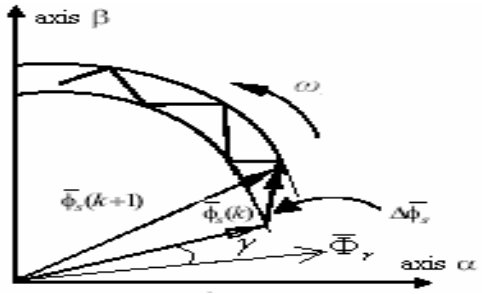

Fig.2. Definition of stator flux increment

The torque is produced by the induction motor can be expressed as equation:

$$Ce = p\frac{M}{\sigma L_s L_r}\Phi_s \Phi_r \sin\gamma \quad \textbf{(5)}$$

The torque depends upon the amplitude of the two vectors stator flux $\overline{\Phi}_s$ and rotor flux $\overline{\Phi}_r$, and their relative position γ. If one succeeds in perfectly controlling the flux $\overline{\Phi}_s$ (starting with Vs) in module and in position, one can subsequently control the amplitude and the relative position of Φ_r and therefore ultimately, the torque.
The choice of stator vector tension depends the desired variation for the module of stator flux, upon its rotation sense and finally upon of the desired evolution for the torque. Through the components of stator flux indicated by the reference point (α,β) bound to the stator, one can decompose the space of Φ_s, into six various zones, or sectors:

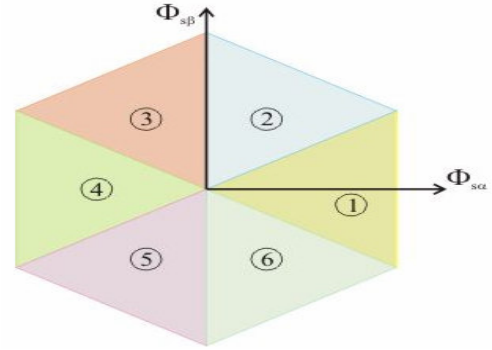

Fig.3. (α,β) plane division in six angular sectors Si (i=1…6)

The level of efficiency of the tension vectors applied to the motor depends upon the position of the vector of stator flux in the i zone.

3. Three level converter

Figure 4 presents the basic structure of a three–level neutral-point-clamped converter. Each of three legs of the converter consists of four power switches, four freewheeling diodes and two clamping diodes that limit the voltage excursions across each device to half the input DC-bus voltage.

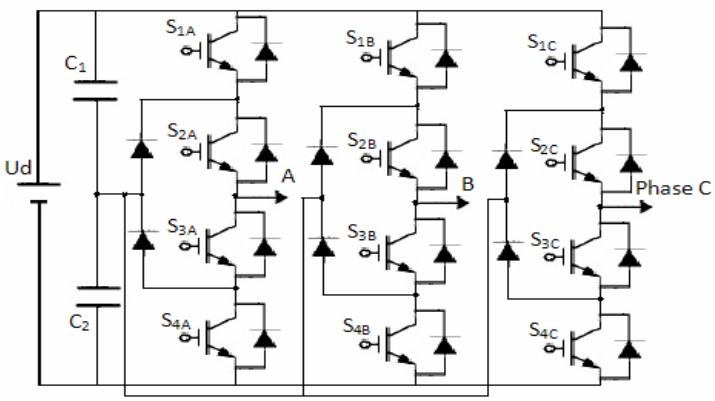

Fig.4. Basic structure **of** three level diode clamped converter

By following the states of conduction of the switches at every arm of the converter, the output voltage can take three values to know: - Ud/2, 0 and +Ud/2 corresponding respectively to the states -1, 0 and +1 of the order size Boolean's.

Table 1 shows the switching states available for the three level converters of Figure 4. There are nineteen basic space vectors for a three-level converter and they are shown in figure 5. The zero voltage vector (V1) has three switching states (000, 111, -1-1-1). Each of the six small vectors (V2—V7) has two switching states and each of the middle vectors (V9, V11, V13, V15, V17) and the large vectors (V8, V10, V12, V14, V16, V18) has one state respectively.

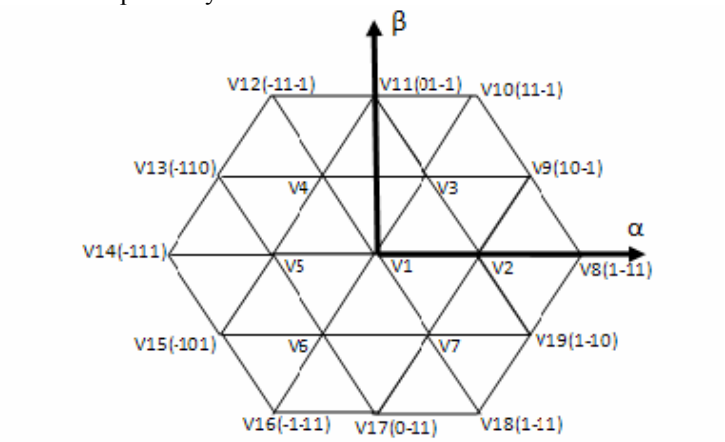

Fig.5. Switching states of converter

4. Speed estimation with MRAS

In this section we present the structure of the observer under study, which is based on the induction motor model written in stator reference frame [3].The state equation of the induction motor can be expressed as follows:

$$\begin{cases} \dot{X} = A.X + B.U \\ Y = C.X \end{cases} \quad \textbf{(6)}$$

Where

$$X = \begin{bmatrix} i_{s\alpha} & i_{s\beta} & \varphi_{r\alpha} & \varphi_{r\beta} \end{bmatrix}^t \quad ; \quad U = \begin{bmatrix} V_{s\alpha} \\ V_{s\beta} \end{bmatrix} \quad ; \quad Y = \begin{bmatrix} i_{s\alpha} \\ i_{s\beta} \end{bmatrix}$$

$$A = \begin{pmatrix} -\left(\frac{1}{\sigma T_s} + \frac{1-\sigma}{\sigma T_r}\right) & 0 & \frac{1-\sigma}{\sigma M T_r} & \frac{1-\sigma}{\sigma M}\omega \\ 0 & -\left(\frac{1}{\sigma T_s} + \frac{1-\sigma}{\sigma T_r}\right) & -\frac{1-\sigma}{\sigma M}\omega & \frac{1-\sigma}{\sigma M T_r}\omega \\ \frac{M}{T_r} & 0 & -\frac{1}{T_r} & -\omega \\ 0 & \frac{M}{T_r} & \omega & -\frac{1}{T_r} \end{pmatrix}$$

$$B = \begin{pmatrix} \frac{1}{\sigma L_s} & 0 \\ 0 & \frac{1}{\sigma L_s} \\ 0 & 0 \\ 0 & 0 \end{pmatrix} \quad \text{et} \quad C = \begin{pmatrix} 1 & 0 & 0 & 0 \\ 0 & 1 & 0 & 0 \end{pmatrix}$$

ω is the rotor mechanical speed.
R_s and L_s are the stator resistance and the cyclic inductance, R_r and L_r are the rotor resistance and the cyclic inductance, M is the mutual inductance, p is the number of pole pairs, σ is the leakage coefficient, with:
$T_s=L_s/R_s$, $T_r=L_r/R_r$, $\sigma=1-M^2/(L_s.L_r)$

A linear state observer for the rotor flux can then be derived as follows by considering the mechanical speed as a constant parameter since its variations are very slow in comparison the electrical variables.
The symbol ˆ denotes an estimated quantity.

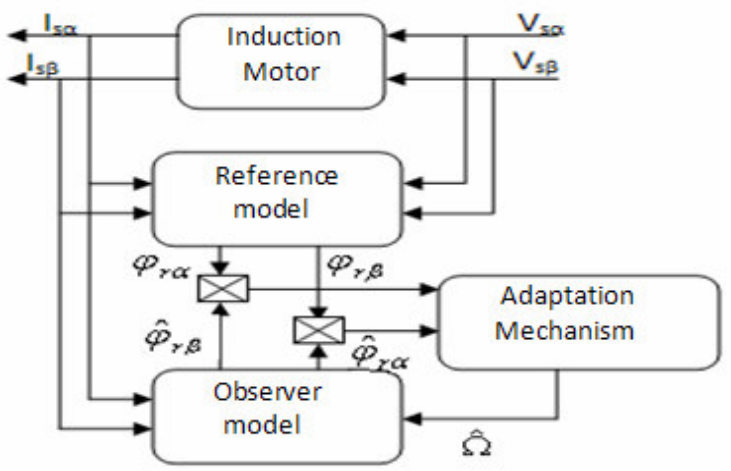

Fig.6. Adaptive observer structure

The reference model is a model that doesn't depend on the rotation speed; it allows calculate the components of rotor flux from the equations of the stator voltage:

$$\frac{d\varphi_{r\alpha}}{dt} = \frac{L_r}{M}\left(V_{s\alpha} - R_s I_{s\alpha} - \sigma L_s \frac{dI_{s\alpha}}{dt}\right)$$
$$\frac{d\varphi_{r\beta}}{dt} = \frac{L_r}{M}\left(V_{s\beta} - R_s I_{s\beta} - \sigma L_s \frac{dI_{s\beta}}{dt}\right) \quad \textbf{(7)}$$

The observer model uses the speed of rotation in his equations and permits to estimate the components of rotor flux:

$$\frac{d\hat{\varphi}_{r\alpha}}{dt} = -\frac{1}{T_r}\varphi_{r\alpha} - p\hat{\Omega}\varphi_{r\beta} + \frac{M}{T_r} I_{s\alpha}$$
$$\frac{d\hat{\varphi}_{r\beta}}{dt} = -\frac{1}{T_r}\varphi_{r\beta} + p\hat{\Omega}\varphi_{r\alpha} + \frac{M}{T_r} I_{s\beta} \quad \textbf{(8)}$$

The adaptation mechanism compares the two models and estimates the speed of rotation by an integral proportional regulator.

Using Lyapunov stability theory, we can construct a mechanism to adapt the mechanical speed from the asymptotic convergence's condition of the state variables estimation errors.

$$\hat{\Omega} = Kp(\hat{\varphi}_{r\alpha}\varphi_{r\beta} - \varphi_{r\alpha}\hat{\varphi}_{r\beta}) + Ki\int(\hat{\varphi}_{r\alpha}\varphi_{r\beta} - \varphi_{r\alpha}\hat{\varphi}_{r\beta})dt \quad \textbf{(9)}$$

Kp and Ki: are positive gains.

5. Correction of the system

5.1. Correction of the stator flux

One may use a two-level comparison of hysteresis. Its aim is the maintain the extremity of the vector of stator flux in one circular crown. Corrective measures, represented by a Boolean variable, indicate if the amplitude of the flux must be increased (δ=1) or decreased (δ=0) in order to maintain:

$$\left| \Phi_{sref} - \Phi_s \right| \leq \Delta\Phi_s \quad \textbf{(10)}$$

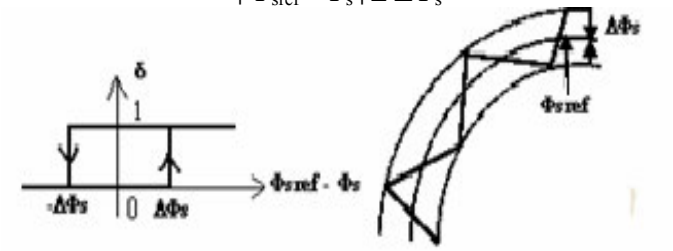

Fig.7. Two level hysteresis comparator

5.2. Correction of the torque

One uses a comparison of hysteresis up to three levels (-1,0,1), which permits the control of the motor in both senses of rotation, and therefore, both the positive and negative torque. The exit from corrective measures generates a Boolean variable (μ=-1) to reduce the torque, (μ=0) to maintain its constant in a ΔC strip around its reference, and (μ=1) to increase the torque. This correction assures to operate in all four quadrants:

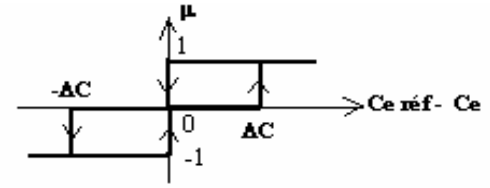

Fig.8. Three level hysteresis comparator

5.3. Correction of speed

The PI (proportional integral) regulator is used to annul the static error and to reduce the response time while maintaining the stability of the system. The method of retaining PI synthesis regulator is that of pole compensation.
The loop of speed can be represented by:

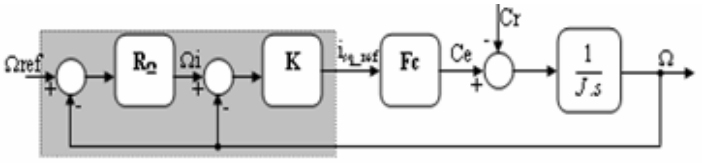

Fig.9. Functional diagram of the control of the speed

Where [7],

$$C_e(s) = p\frac{L_s}{M}.(1-\sigma).\Phi_{r\_réf}.\frac{1}{1+\tau_{bf}.s}i_{sq\_réf}(s) = Fc(s).i_{sq\_réf}(s) \quad \textbf{(11)}$$

With

$$Fc(s) = \frac{1.6}{1+\tau_{bf}.s}, \tau_{bf} = \frac{\sigma L_s}{10R_{sr}}, R_{sr} = R_s + (\frac{M}{L_r})^2 R_r$$

The reference of rotor flux of our application is fixed to 0.8Wb what corresponds in regime permanent to a reference of Flux statorique of 0.85Wb, found by the relation of equivalence between the reference of the stator flux and that of the rotor flux can be deducted by the equations of the induction motor steady-state model :

$$\Phi_s = \frac{L_s}{M}\Phi_r\sqrt{\left(1+(\sigma.Tr.\omega_{sl})^2\right)} \quad \textbf{(12)}$$

ω_{sl} is the difference between the angular speed of the reference frame and the electrical speed ω of the rotor.

The first loop to proportional action (K) retains the principal loop of speed as a system of the second dominant order, adjusted for the optimized amortization. The parameters of the P-PI regulator are then:

[K=13.75- K_Ω=400-τ_Ω=1.5ms]

5.4. High speed range

In the high-speed one adopts the weakening of flux.

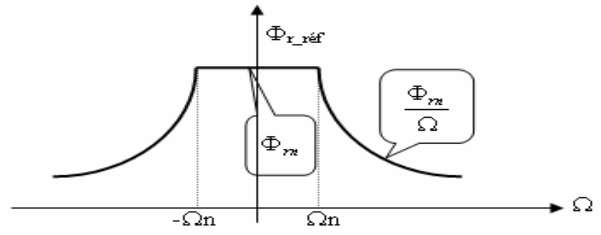

Fig.10. Reference rotor flux law

With Ωn: nominal value of rotor speed, Φ_m: nominal value of the rotor flux.
So the reference of stator flux can be found from this law and the equation (12).

6. Simulation results

For the control schemes that operate at a fixed switching frequency, an inverter switching frequency of 10 KHz was used. For the DTFC simulations, torque and flux hysteresis bands of 0.2Nm and 0.01Wb respectively.

6.1. Regulation of speed mode

The load torque is fixed of 20Nm and the maximal electromagnetic torque is limited to 1.6Cn. One imposes a speed of reference varying from between -955 rpm and +955 rpm:

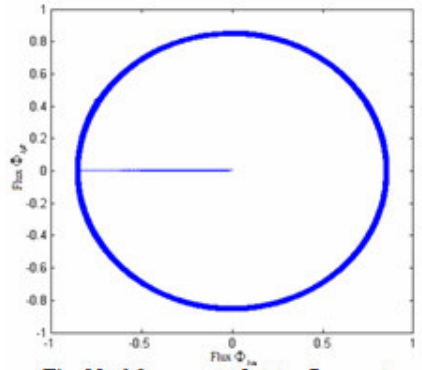

Fig. 11. Movement of stator flux vector

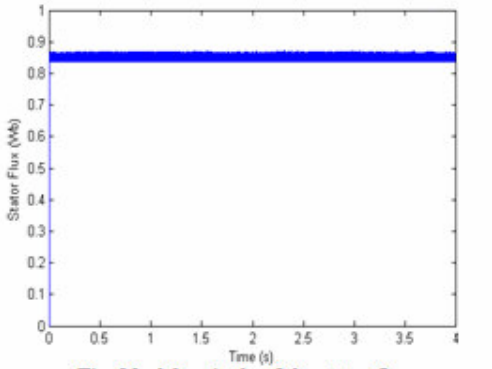

Fig. 12. Magnitude of the stator flux

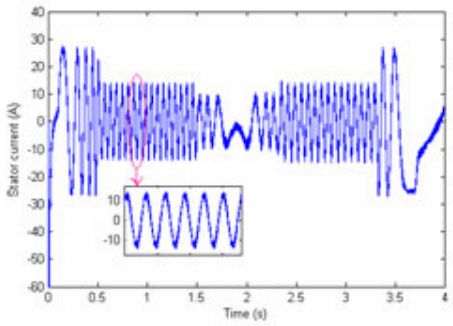

Fig. 13. Phase stator current

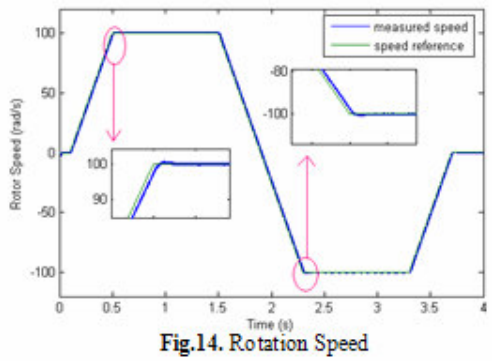

Fig.14. Rotation Speed

6.2 High speeds mode

We keep the same condition of the speed control and impose a rotor speed of 1910 rpm:

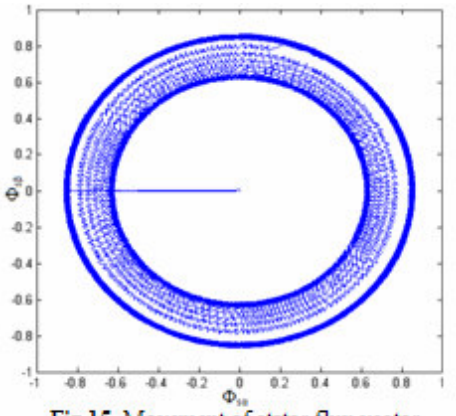

Fig.15. Movement of stator flux vector

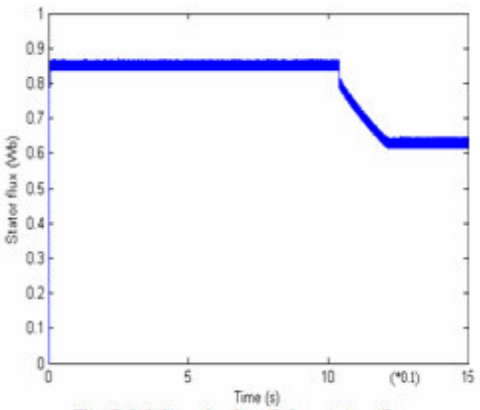

Fig.16. Magnitude of the stator flux

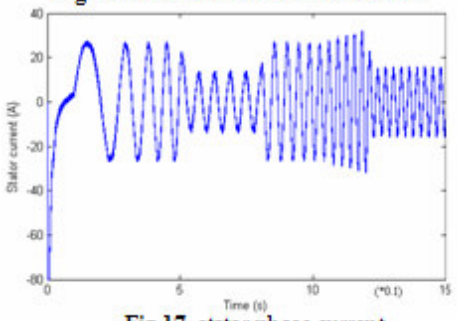

Fig.17. stator phase current

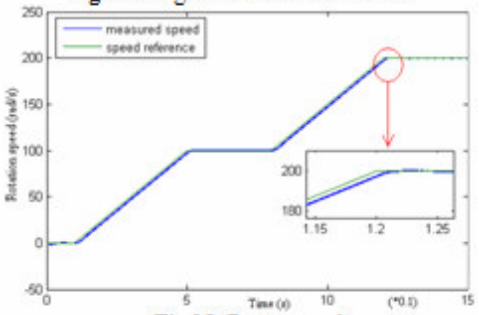

Fig.18. Rotor speed

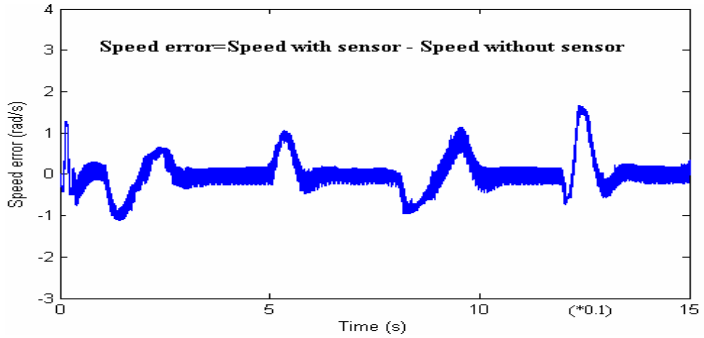

Fig.19. Error speed

6.3 Low speeds

We keep the conditions of the previous test and verified the working to low speed between 5rad/s and -5rad/s:

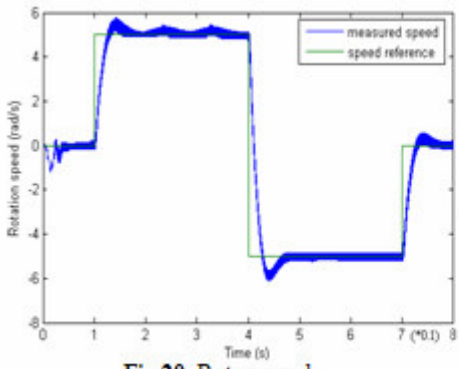

Fig.20. Rotor speed

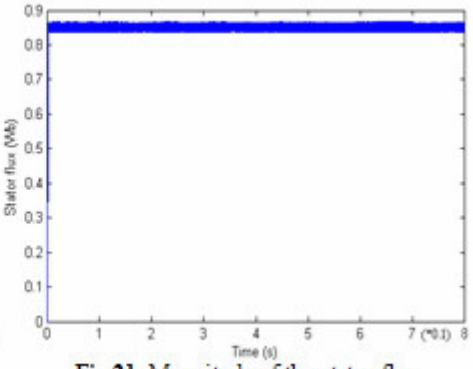

Fig.21. Magnitude of the stator flux

The following results are done by simulation with MATLAB/Simulink software. With the results we can estimate the rotor speed in the different working of low speeds to the high speeds. The speed error calculated from the difference between speed with sensor and speed without sensor remain weak and remains bellow ±1.5 rad/s. The dynamics of flux and the torque are better and the ripples are reduced. The current in the induction motor remains sinusoidal and takes appropriate values even in high speeds.

7. Conclusion

In this paper we have studied the remarkable performances of an induction motor drive technique using the Sensorless DTFC strategy associated with the three levels neutral point clamped converter. We proposed an adaptive method of evaluation of the speed of the valid even in high speed. The diagram of the control proposed allows reducing the ripples of flux and torque and especially improving the performances of the DTFC order in high and low speed. Also a converter three levels give better results than the converter two levels while reducing the THD of the out current.The DTFC strategy is simple and offers the advantage to uses voltage and current measurements only and don't need any speed or position encoders. It has also a faster dynamic response due to the absence of PI current regulator

References

1. J. Belhadj, I. Slama-Belkhodja, M. Pietrzak-David and B. De Fornel, ″Direct Torque control of induction machine with a short-time computing observer″, Electromotion Vol.10 pp.449-454, Marrakesh, Morocco, 2003.

2. P. Purkait and R. S. Sriramkavacham, ″A New Generalized Space Vector Modulation Algorithm for Neutral-point-clamped Multilevel Converters″, *Electromagnetics Research Symposium*, Cambridge, USA, 2006, March 26-29, pp. 330-335.

3. J.-P. Caron et J.-P. Hautier, "Modélisation et commande de la machine asynchrone", Editions Technip, Paris, 1995.

4. R. Ortega, N. Barabanov and G. Escobar, ″Direct torque control of induction motors: stability analysis and performance improvement″, *IEEE Trans. Automat. Contr.*, Vol. 46, Aug. 2001, pp. 1209-1222.

5. V.Cecconim, M.Cirrincione, D.La Cascia,M.Pucci and P.Zito,″A New optimal efficiency Direct Torque Control induction motor drive for electric vehicles″, Electromotion Vol.10,pp.317-324,Marrakesh, Morocco, 2003.

6. Petar R.Matic, Branko D.Blanusa and Slobodan N. Vukosavic,″A Novel Direct Torque and Flux Control algorithm for the Induction Motor drive″, IEEE trans.Ind.App. pp.965-970, 2003.

7. A. Abbou and H. Mahmoudi, ″Etude d'une commande vectorielle à flux rotorique orienté avec et sans capteur mécanique du moteur asynchrone piloté par une commande MLI intersective optimisée″, JTEA'06, 4th International Conference, 12-14 May, Tunis 2006.

8. D. Casadei and G.Serra, ″Implementation of Direct Torque Control algorithm for induction motors based on Discrete Space Vector Modulations″, IEEE trans .Power Electronics, vol.15, N°4, July 2002.

9.Takahashi and T. Noguchi, "a new quick response and high-efficiency control strategy of induction motor," IEEE Trans. I.A, vol.22, n°5, 1987, pp.820-827.

Appendix

Etats	S_{1X}	S_{2X}	S_{3X}	S_{4X}
1	ON	ON	OFF	OFF
0	OFF	ON	ON	OFF
-1	OFF	OFF	ON	ON

Table 1. Switching states of three-level converter (X=A,B,C)

Rated output power	7.5 KW
Rated voltage	380 V Y
Rated frequency	50 Hz
Pole-pair number	2
Rated speed	1450 rpm
Stator resistance	0.63 Ω
Rotor resistance	0.4 Ω
Stator Leakage Inductance	97 mH
Rotor Leakage Inductance	91 mH
Mutual Inductance	91 mH
Moment of inertia	0.22 $Kg.m^2$

Table 2. Induction Motor Parameters